Study of the v6 band of CH3Br by infrared laser sideband and submillimeterwave spectroscopy

J. M. Chevalier, J. Legrand, P. Glorieux, G. Wlodarczak, and J. Demaison

Citation: J. Chem. Phys. **90**, 6833 (1989); doi: 10.1063/1.456256
View online: http://dx.doi.org/10.1063/1.456256
View Table of Contents: http://jcp.aip.org/resource/1/JCPSA6/v90/i12
Published by the AIP Publishing LLC.

Study of the ν_6 band of CH_3Br by infrared laser sideband and submillimeter-wave spectroscopy

J. M. Chevalier, J. Legrand, P. Glorieux, G. Wlodarczak, and J. Demaison
Laboratoire de Spectroscopie Hertzienne, associé au CNRS, Université de Lille I, 59655 Villeneuve d'Ascq Cedex, France

(Received 15 December 1988; accepted 23 February 1989)

About 136 transitions in the ν_6 band of CH_3Br have been measured using an infrared laser sideband spectrometer. The sidebands were generated by mixing the 10 μm radiation of a CO_2 laser with the radiation of a tunable high power microwave source. Frequencies of transitions with $J \leqslant 71$ and $K \leqslant 8$ are reported. The accuracy of the measurements is estimated to be better than 10 MHz. Some high J rotational transitions in the $v_6 = 1$ state have also been measured with a submillimeter-wave spectrometer. The new measurements have been combined with previous results to derive vibration–rotation parameters for the $v_6 = 1$ state.

INTRODUCTION

A large number of studies have already been devoted to the rotational and rovibrational spectra of methyl bromide (CH_3Br). See Ref. 1 for an extensive review of the work prior to 1981. Particularly the constants of the ground state and the $v_6 = 1$ state have been determined by a combined analysis of the rotational spectra (in the $v = 0$ and $v_6 = 1$ states) and the infrared transitions from Doppler free saturation spectroscopy.[2] The laser Stark data of Ieki *et al.*[3] have also been included. But the microwave spectra were limited to 240 GHz and only a small number of infrared transitions could be measured due to the lack of tunability of the spectrometer. Therefore, the statistical determination of some parameters was questionable and other parameters could not be accurately determined.

Since that time it has become much easier to measure submillimeter-wave rotational spectra and new infrared laser spectrometers have been developed which permit us to measure in a much wider frequency range together with a high accuracy in frequency measurement. These technical developments have allowed us to extend measurements in the submillimeter wave as well as in the infrared ranges and justify a new determination of the constants of CH_3Br.

The ground state submillimeter-wave rotational spectrum of CH_3Br was recently measured up to 800 GHz.[4] A merged least-squares fit including the constants obtained from a fit of the infrared ground state combination differences has given very accurate ground state constants.

The $2\nu_6$–ν_6 hot band of CH_3Br was also very recently measured by laser–Stark spectroscopy.[5] In that work the axial rotational constant in the ground state and the centrifugal distortion constants D_K and H_K were determined. Arimondo *et al.* have used the highly sensitive infrared–radio frequency double resonance inside a CO_2–N_2O laser cavity to observe pure nuclear quadrupole resonances and direct A_1–A_2 transitions in CH_3Br.[6] The hyperfine structure of the rotational spectrum was also investigated by Kukolich and Cogley and by Osipov and Grabois.[8]

EXPERIMENTAL TECHNIQUES

The submillimeter-wave spectrum of the $v_6 = 1$ state was measured with a source modulated spectrometer which uses a phase-stabilized submillimeter-wave backward-wave oscillator (BWO) as a source. The submillimeter-wave power is optically focused through a free space absorption cell (1 m length) and detected by helium cooled InSb detector. After phase sensitive detection the signal is digitally averaged and processed by a microcomputer in the usual way. Many transitions appear as doublets because of the interaction of the bromine nuclear moment with the gradient of the molecular electric field at the nucleus position. The measured transitions, given in Tables I and II are corrected for this effect using the hyperfine constants of Ref. 15. The accuracy of the submillimeter measurements is about 100 kHz.

The infrared microwave sideband spectrometer used for measuring the infrared absorption spectrum of CH_3Br is based on the high frequency electro-optic modulation technique which was introduced by Corcoran *et al.*[9,10] in 1970 and fully developed later by Magerl *et al.*[11–13] In this technique, tunable sidebands are generated by tunable microwave modulation of a fixed frequency 10 μm laser radiation.

The modulating microwave field from a YIG oscillator is amplified by a 20 W traveling-wave tube (TWT) and applied to a CdTe crystal inserted in a metallic waveguide. Inside this waveguide a $3 \times 3 \times 40$ mm^3 CdTe crystal is sandwiched between two Al_2O_3 slabs whose dimensions were calculated to achieve velocity matching of the infrared wave and of a microwave radiation at 13 GHz. The crystal housing is set between double ridge waveguide sections.[14] With the polarization and crystal axes chosen in our device, the available sideband power is given by[12]:

$$P_{sb} = (\gamma^2/16)P_c \tag{1}$$

with $\gamma = [2\pi n_0^3 r_{41} E_m L \operatorname{sinc}(\omega_m L/2W)]/\lambda_c$. In this expression P_c and λ_c are the CO_2 laser power and wavelength, respectively, E_m and ω_m the microwave field amplitude and pulsation, respectively, n_0 and r_{41} the infrared refractive index and electro-optic coefficient of CdTe, L the crystal length and W characterizes the phase velocity mismatch between the microwave and IR fields:

$$W^{-1} = V_c^{-1} - V_m^{-1}, \tag{2}$$

where V_c and V_m are the phase velocity of the IR carrier and of the microwave modulation, respectively.

The overall scheme of the spectrometer is given in Fig. 1.

 0021-9606/89/126833-07$02.10

TABLE I. Newly observed $J+1, F+1 \leftarrow J,F$ transitions of $CH_3{}^{79}Br$ in the $\nu_6 = 1$ state. All values in MHz (+) and (−) denote the higher and the lower components of the l-doubling transitions, respectively. $\bar{\nu}$ is the frequency corrected for the hyperfine structure and I the nuclear spin of iodine.

J	Kl	$F=\begin{cases}J+I\\J-I\end{cases}$	$F=\begin{cases}J+I-1\\J-I+1\end{cases}$	$\bar{\nu}$	Obs. − calc.
18	− 9	361 520.224	361 530.476	361 525.350	− 0.045
18	− 8	361 615.737		361 619.800	0.056
18	10		361 645.892	361 639.562	− 0.112
18	9	361 716.608	361 726.626	361 721.617	0.093
18	− 6	361 776.844	361 781.430	361 779.137	0.085
18	8	361 789.675	361 797.836	361 793.756	− 0.013
18	− 5	361 842.325	361 845.637	361 843.981	0.014
18	7	361 853.184		361 856.287	− 0.083
18	1(+)			361 857.096	− 0.225
18	6	361 906.823	361 911.890	361 909.357	0.066
18	5	361 950.950	361 954.060	361 952.503	− 0.006
18	− 2			361 979.478	− 0.051
18	4	361 984.896	361 987.301	361 986.098	0.086
18	− 1			362 004.807	− 0.064
18	0			362 019.947	− 0.002
18	2			362 024.370	0.105
18	1(−)			362 196.632	− 0.098
20	− 11	399 267.421	399 278.807	399 273.114	− 0.045
20	− 10	399 394.334	399 403.611	399 398.973	0.002
20	12	399 421.143		399 427.895	0.043
20	− 9	399 510.322	399 517.850	399 514.086	0.058
20	− 8	399 615.335	399 621.367	399 618.350	0.054
20	10		399 645.120	399 640.421	0.012
20	9	399 727.065	399 734.718	399 730.892	0.023
20	− 6	399 792.735	399 796.040	399 794.388	0.039
20	8	399 807.602	399 812.023	399 810.599	− 0.117
20	− 5	399 864.775	399 867.317	399 866.046	− 0.039
20	7	399 877.714		399 880.003	0.097
20	1(+)			399 881.035	− 0.001
20	6	399 936.674	399 939.872	399 938.273	− 0.129
20	5	399 985.039	399 987.481	399 986.260	0.082
20	− 2			400 015.871	0.016
20	− 1			400 043.739	− 0.074
20	3			400 049.638	0.032
20	0			400 060.367	0.040
20	2			400 065.755	0.053

The radiation coming from a cw CO_2 laser is focused inside the CdTe crystal. The CO_2 laser is locked at the top of its emission mode. The sideband infrared radiation is filtered by crossed polarizers and refocused inside the 80 cm Stark absorption cell. The radiation emerging from that cell is diverging and it is refocused on a HgCdTe detector. Except for wideband recordings (8–18 GHz) such as the one given in Fig. 2, the absorption signal is read by an A.D. converter and stored in the computer. In this spectrometer, on–off Stark modulation at 50 kHz has been applied in order to reduce the possible spurious signals due to residual microwave VSWR (voltage standing wave ratio) effects. The strength of the Stark field is 1500 V/cm typically, which is sufficient to resolve the absorption lines in most cases.

INFRARED SPECTRUM

The ν_6 band of CH_3Br is perpendicular and the corresponding selection rules are $\Delta J = 0, \pm 1, \Delta K = \Delta l = \pm 1$. The application of a Stark field parallel to the polarization of the sidebands implies the $\Delta M = 0$ selection rule. Figure 2 shows a wideband recording (8–18 GHz) of the CH_3Br absorption spectrum when the CO_2 laser is operated on the 10P 16 line. The accuracy of the frequency measurement is usually of the order of 8 MHz. It depends on the signal-to-noise ratio of the absorption signal and on the accuracy of the CO_2 laser locking loop. It will be improved in a future version by locking the laser to the 4.3 μm saturated fluorescence signal.[16] The experimental full width at half-maximum (FWHM) of most lines is 35 MHz, i.e., equal to the calculated Doppler width. Some lines are wider which may be explained by the nuclear quadrupole hyperfine structure. On the contrary in the (8–11.5 GHz) frequency band, many lines have a FWHM equal to half the Doppler width. In fact, these lines correspond to absorptions of the microwave second harmonic sideband. The efficiency of the electro-optic modulator for the second harmonic generation is much too weak to explain these results. Similarly, the level of second harmonic generated by the TWT amplifier, which is to − 50 dBc, is by far too low. On the other hand, the generation of second harmonic by the YIG source and the PIN modula-

TABLE II. Newly observed $J+1, F+1 \leftarrow J, F$ transitions of $CH_3{}^{81}Br$ in the $\nu_6 = 1$ state. All values in MHz. (+) and (−) denote the higher and the lower components of the *l*-doubling transitions, respectively. $\bar{\nu}$ is the frequency corrected for the hyperfine structure and I the nuclear spin of iodine.

J	Kl	$F=\begin{cases}J+I\\J-I\end{cases}$	$F=\begin{cases}J+I-1\\J-I+1\end{cases}$	$\bar{\nu}$	Obs. − calc.
18	− 10	360 046.986	360 055.828	360 050.649	− 0.015
18	12	360 069.914	360 086.842	360 076.917	− 0.133
18	− 9	360 149.971	360 158.314	360 154.126	0.095
18	11	360 170.881	360 184.012	360 177.447	0.236
18	− 8	360 244.307	360 251.266	360 247.787	0.058
18	10	360 262.754	360 273.339	360 268.047	0.097
18	− 7	360 329.032	360 334.281	360 331.657	− 0.068
18	9	360 344.998	360 353.308	360 349.153	− 0.060
18	8	360 417.542	360 424.339	360 420.940	− 0.009
18	− 5	360 469.094	360 471.931	360 470.513	0.011
18	7	360 480.542	360 483.866	360 483.129	0.015
18	1(+)			360 483.858	− 0.024
18	− 3			360 570.250	0.082
18	5	360 577.369	360 580.273	360 578.822	0.233
18	− 2			360 605.432	0.160
18	− 1			360 630.353	− 0.130
18	3			360 635.342	− 0.164
18	0			360 645.425	− 0.074
18	2			360 649.785	− 0.030
18	1(−)			360 821.128	− 0.081
20	12		397 918.925	397 913.694	− 0.077
20	− 9	397 995.584	398 001.964	397 998.774	− 0.005
20	11	398 019.859	398 029.263	398 024.561	0.091
20	− 8	398 099.802	398 104.867	398 102.335	0.003
20	10	398 120.816	398 128.588	398 124.702	− 0.056
20	− 6	398 275.633	398 278.690	398 277.162	− 0.074
20	− 5	398 347.456	398 349.635	398 348.545	0.019
20	7	398 360.557		398 362.474	− 0.098
20	1(+)			398 363.634	0.187
20	6	398 291.434	398 296.473	398 420.645	− 0.022
20	− 3			398 458.810	0.156
20	5	398 467.142	398 469.267	398 468.205	0.090
20	− 2			398 497.330	− 0.098
20	− 1			398 525.335	0.093
20	3			398 531.188	0.096
20	0			398 541.753	0.063
20	2			398 546.960	− 0.095
20	1(−)			398 736.069	− 0.035

tor, which stabilizes its level, and its amplification by the TWT may explain the observed signal. This effect may be enhanced by a shift of the microwave frequency for which perfect phase velocity matching is obtained. For instance, an air gap of 30 μm between the modulator consisting of the CdTe crystal and the Al_2O_3 slabs, and the housing shifts the central tuning frequency to higher frequency and consequently increases the efficiency of the modulator in the high frequency range. Practically, this increases the spectrometer bandwidth, but requires some additional care in the assignment. It can also cause overlapping of absorption lines. Additional filtering using a Fabry–Perot interferometer should be desirable for the study of molecules possessing many absorption lines for which this overlapping could be a problem. Frequency measurements are summarized in Tables III and IV with the corresponding assignments.

ANALYSIS

The vibrational and rotational frequencies were fit to differences in energy levels. For the ground vibrational state the rotational energy may be written:

$$\begin{aligned} E = {} & BJ(J+1) + (A-B)K^2 - D_J J^2(J+1)^2 \\ & - D_{JK} J(J+1)K^2 - D_K K^4 \\ & + H_J J^3(J+1)^3 + H_{JK} J^2(J+1)^2 K^2 \\ & + H_{KJ} J(J+1)K^4 + H_K K^6. \end{aligned} \tag{3}$$

For the $v_6 = 1$ state the diagonal element of the vibration–rotation Hamiltonian is

$$\begin{aligned} \langle JKI|H|JKI\rangle = {} & \nu_6 + BJ(J+1) + (A-B)K^2 - 2A\zeta Kl - D_J J^2(J+1)^2 - D_{JK} J(J+1)K^2 - D_K K^4 \\ & + H_J J^3(J+1)^3 + H_{JK} J^2(J+1)^2 K^2 + H_{KJ} J(J+1)K^4 + H_K K^6 \\ & + \eta_J J(J+1)Kl + \eta_K K^3 l + \eta_{JJ} J^2(J+1)^2 Kl + \eta_{JK} J(J+1)K^3 l. \end{aligned} \tag{4}$$

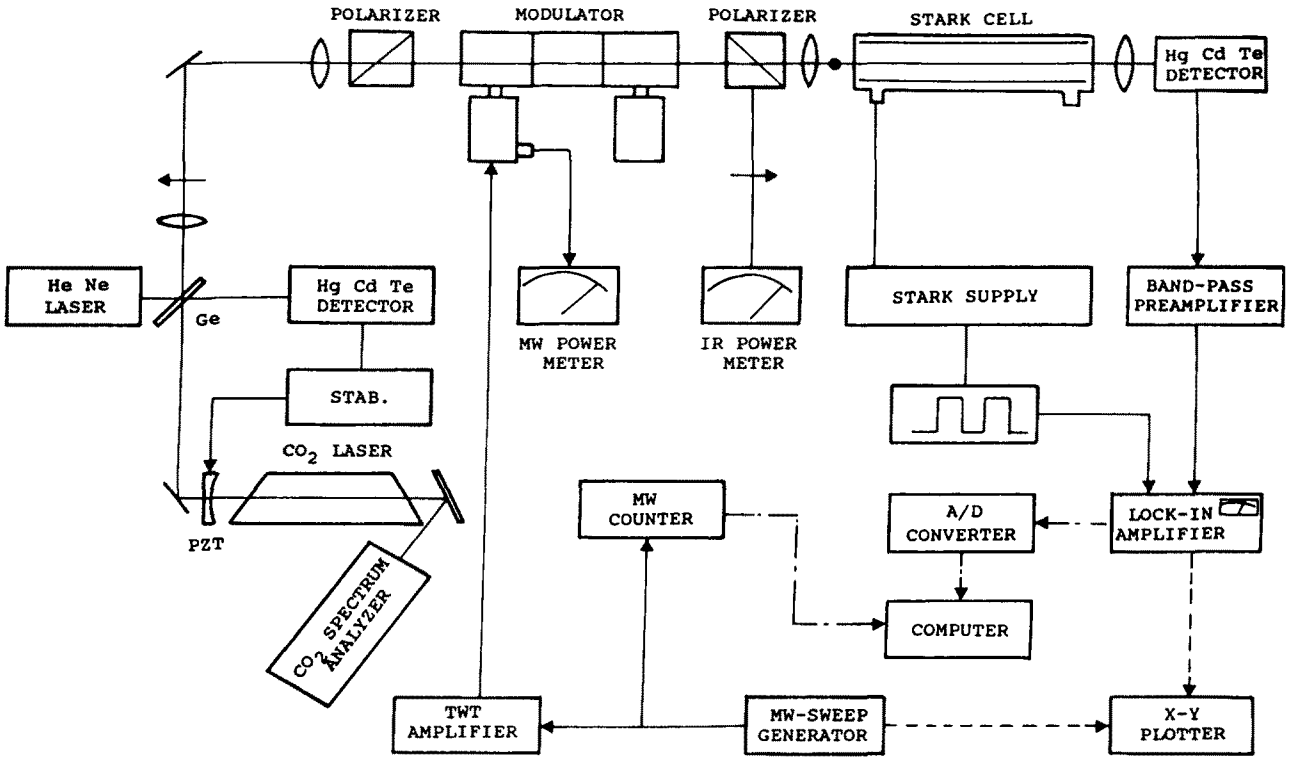

FIG. 1. Block diagram of the sideband laser spectrometer for linear spectroscopy of CH_3Br. The arrows and the point represent the respective polarizations of the carrier and of the sidebands. The dashed lines correspond to wideband recordings and the point dash lines to narrowband recordings.

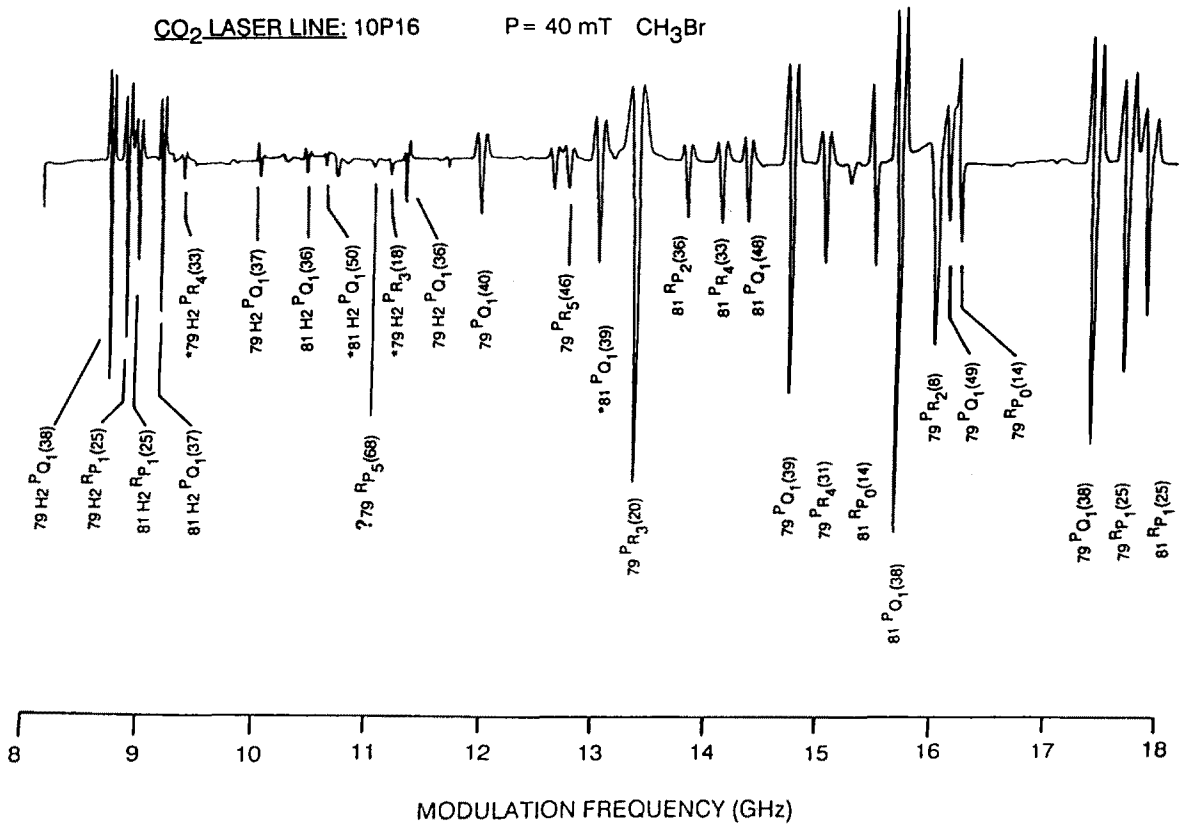

FIG. 2. Recording of CH_3Br absorption signals when the CO_2 laser is operated on 10*P* 16 line. The microwave generator sweeps the 8–18 GHz range. The gas pressure is 40 mT and the time constant 30 ms. The assigned transitions belong to the ν_6 bands of $CH_3{}^{79}Br$ and $CH_3{}^{81}Br$. The H2 symbol means that the transition has been measured on the second harmonic of the MW sweep generator. *: Transition assigned but not measured.

TABLE III. Observed frequencies in the ν_6 band of $CH_3{}^{79}Br$. All values in MHz. Obs. − calc. = observed − calculated frequency.

Transition	F exp	Obs. − calc.	Transition	F exp	Obs. − calc.
$PQ(23;5)$	27 588 668	2	$PR(14;3)$	28 318 814	−3
$PP(12;4)$	27 588 823	5	$PQ(49;1)$	28 396 586	8
$PQ(21;5)$	27 591 742	−2	$PR(31;4)$	28 397 681	−7
$PP(21;3)$	27 624 343	−4	$PQ(40;1)$	28 424 446	13
$PP(18;3)$	27 685 503	−2	$PR(46;5)$	28 425 199	−13
$PQ(48;4)$	27 742 296	7	$PR(20;3)$	28 425 835	22
$PR(18;6)$	27 744 384	6	$PQ(39;1)$	28 427 177	−0
$PQ(47;4)$	27 745 600	12	$PR(8;2)$	28 428 477	6
$PP(15;3)$	27 746 089	4	$RP(14;0)$	28 428 670	−2
$PP(36;1)$	27 750 412	8	$PQ(38;1)$	28 429 846	−7
$PR(23;6)$	27 832 213	9	$RP(25;1)$	28 430 122	−12
$PP(32;1)$	27 835 569	−4	$PQ(37;1)$	28 432 473	15
$RP(42;0)$	27 836 358	12	$PQ(36;1)$	28 435 005	11
$PQ(71;3)$	27 864 360	−6	$PR(12;2)$	28 501 831	11
$PP(9;3)$	27 865 492	1	$RP(43;3)$	28 502 287	9
$PR(25;6)$	27 866 814	−1	$PR(39;4)$	28 529 504	6
$PR(13;5)$	27 868 066	−5	$PR(26;3)$	28 530 173	10
$RP(50;1)$	27 893 212	5	$RP(31;2)$	28 531 317	11
$PP(29;1)$	27 898 819	15	$PR(53;5)$	28 532 410	−2
$PP(17;2)$	27 924 981	9	$RP(20;1)$	28 532 991	2
$PQ(50;3)$	27 952 829	7	$RP(52;4)$	28 533 856	10
$PQ(41;3)$	27 981 267	14	$PR(30;3)$	28 598 230	−1
$PP(25;1)$	27 982 252	9	$RP(49;4)$	28 600 559	3
$PQ(40;3)$	27 984 079	16	$PR(32;3)$	28 631 813	4
$PP(14;2)$	27 985 375	15	$RP(37;3)$	28 632 074	6
$PR(32;6)$	27 985 587	9	$RP(15;1)$	28 634 269	6
$PQ(39;3)$	27 986 819	14	$RP(26;2)$	28 636 027	9
$PQ(38;3)$	27 989 481	3	$PR(33;3)$	28 648 479	−3
$PR(15;4)$	28 119 507	−5	$PR(8;1)$	28 649 615	4
$PP(7;2)$	28 123 980	−3	$RP(36;3)$	28 653 500	7
$PP(18;1)$	28 125 842	5	$RP(24;2)$	28 677 476	6
$PR(17;4)$	28 155 304	−14	$PR(22;2)$	28 680 160	0
$RP(38;1)$	28 155 514	−17	$RQ(27;0)$	28 681 116	−6
$PQ(54;2)$	28 157 617	−2	$PR(35;3)$	28 681 599	1
$PQ(36;2)$	28 213 871	5			

The l-doubling off-diagonal element has also to be taken into account:

$$\langle JKl|H|JK\pm 2, l\pm 2\rangle = \tfrac{1}{2}\{q_0 - q_1 J(J+1)\} \times\{J(J+1) - K(K\pm 1)\}^{1/2} \times\{J(J+1) - (K\pm 1)(K\pm 2)\}^{1/2}. \quad (5)$$

This off-diagonal element may be treated by perturbation or by diagonalization of a 2×2 matrix. In the case of CH_3Br, the ratio $q^2/(A - B - A\zeta)$ is small, so that the largest difference between the results of the perturbation and of the diagonalization is only some hundreds of kHz, i.e., at least an order of magnitude smaller than the experimental accuracy.

The axial rotational constant A is not determinable from our measurements. Furthermore, the distortion constants D_K and η_K are not separately determinable; only the combinations $\nu_6 + A' - B' - 2A'\zeta + (3/4)\eta_K$, $A' - B' - A'\zeta + \eta_K$, $A' - A'' - (B' - B'') + (3/2)\eta_K$, $D'_K - \eta_K/4$, and $D''_K - \eta_K/4$ may be obtained.[17]

In all the least-squares fittings the weight assigned to each experimental frequency was the inverse of the square of the uncertainty in the measured value. In a first weighted least-squares fit we took into account all the experimental data listed in Table V. Only the lines which could be assigned without ambiguity were retained in the final least-squares fit. The derived ground state rotational constants are identical to those of Ref. 4, but slightly less accurate. Furthermore, the correlations between the ground state constants and the other parameters are small. In the following (and final) fits we have fixed the ground state constants at the values of Ref. 4. The corresponding constants are listed in Table VI. Nearly all the parameters are well determined. Specifically, only two correlation coefficients are greater than 0.9:

$\rho(D_J, H_J) = 0.955$ for $CH_3{}^{79}Br$ and 0.927 for $CH_3{}^{81}Br$

$\rho(D''_K - \eta_K/4, D'_K - \eta_K/4) = 0.991$

for $CH_3{}^{79}Br$ and 0.909 for $CH_3{}^{81}Br$.

However, the constants H_{JK} do not seem coherent with ground state values and their isotopic dependence is very large. They should be considered as fitting parameters. An attempt to determine the sextic constants H_K was not successful, the ratio $H_K/\sigma(H_K)$ being only about equal to 2, either for the ground state or for the $v_6 = 1$ excited state. To

TABLE IV. Observed frequencies in the ν_6 band of $CH_3{}^{81}Br$. All values in MHz. Obs. − calc. = observed − calculated frequency.

Transition	*F* exp	Obs. − calc.	Transition	*F* exp	Obs. − calc.
PP(12; 4)	27 587 460	− 0	*PQ*(47; 2)	28 180 474	5
PQ(21; 5)	27 589 449	− 4	*PP*(4; 2)	28 180 669	4
PQ(19; 5)	27 592 247	1	*PQ*(46; 2)	28 183 695	10
PR(10; 6)	27 596 863	37	*PQ*(37; 2)	28 209 520	18
PR(13; 6)	27 651 290	14	*PQ*(35; 2)	28 214 483	3
PP(18; 3)	27 684 720	3	*PP*(10; 1)	28 284 921	7
PQ(55; 4)	27 715 414	2	*PR*(38; 5)	28 292 891	3
PQ(47; 4)	27 743 660	7	*RP*(41; 2)	28 318 945	0
PP(4; 4)	27 743 956	5	*PP*(8; 1)	28 324 178	3
PP(15; 3)	27 745 070	4	*PP*(7; 1)	28 343 719	13
PR(36; 7)	27 835 277	11	*PQ*(48; 1)	28 398 370	0
PP(32; 1)	27 836 108	− 4	*PP*(4;1)	28 401 915	12
PR(51; 8)	27 861 537	− 3	*RP*(36; 2)	28 426 256	− 1
PR(25; 6)	27 862 573	5	*PR*(33; 4)	28 426 557	− 5
PP(20; 2)	27 863 492	9	*RP*(14; 0)	28 427 912	1
PR(13; 5)	27 864 730	2	*PQ*(38; 1)	28 428 149	5
PR(38; 7)	27 867 736	− 17	*RP*(25; 1)	28 430 319	− 9
PR(27; 6)	27 896 758	8	*PQ*(37; 1)	28 430 744	5
RP(70; 3)	27 897 101	− 11	*PQ*(36; 1)	28 433 273	9
PP(17; 2)	27 924 229	12	*PR*(12; 2)	28 498 883	10
RP(38; 0)	27 925 464	− 13	*RP*(31; 2)	28 532 091	8
PQ(50; 3)	27 951 050	10	*RP*(20; 1)	28 532 796	6
PQ(40; 3)	27 982 169	15	*PR*(14; 2)	28 534 986	3
RP(46; 1)	27 983 472	5	*RP*(49; 4)	28 603 028	3
PP(14; 2)	27 984 388	13	*PR*(44; 4)	28 604 122	2
PQ(39; 3)	27 984 898	14	*PR*(32; 3)	28 627 438	1
PQ(38; 3)	27 987 548	1	*PR*(7; 1)	28 628 607	− 0
PQ(37; 3)	27 990 146	7	*RP*(37; 3)	28 633 443	6
PP(7; 2)	28 122 473	3	*RP*(15; 1)	28 633 690	11
PP(18; 1)	28 125 272	3	*RP*(58; 5)	28 634 114	− 2
PR(28; 5)	28 127 264	15	*RP*(24; 2)	28 677 697	7
PR(41; 6)	28 127 462	− 14	*RQ*(25; 0)	28 682 521	− 3
PQ(54; 2)	28 156 003	− 7	*PR*(10; 1)	28 683 730	− 1
RP(38; 1)	28 156 771	− 0			

TABLE V. Sources of data for CH_3Br.

Experiment	Source	Transitions	Uncertainty
IR–MW sideband laser	this work Tables III and IV	high and low *J*,*K*	8 MHz
IR saturation laser	Ref. 2	high and low *J*, *K*	500 kHz
IR laser stark	Ref. 3 Tables I–IV[a]	low *J*	10 MHz
SMM wave	this work Tables I and II	$\nu_6 = 1$ $J = 18, 20$; $K \leqslant 12$	100 kHz
MW and MMW	Ref. 18 Tables III and IV	$\nu_6 = 1$ $0 \leqslant J \leqslant 11$; $K \leqslant 7$	30 to 100 kHz
SMM Wave	Ref. 4 Table I	$\upsilon = 0$ $13 \leqslant J \leqslant 40$; $K \leqslant 12$	50 to 200 kHz
MMW beam absorption	Ref. 19 Tables I and II	$\upsilon = 0$ $3 \leqslant J \leqslant 11$; $K \leqslant 3$	1 to 5 kHz
MW and MMW	Ref. 20 Table III	species 79, $\upsilon = 0$ $6 \leqslant J \leqslant 12$; $K \leqslant 12$	100 kHz
MW and MMW	Ref. 21 Table I	species 81, $\upsilon = 0$ $0 \leqslant J \leqslant 15$; $K \leqslant 12$	100 kHz

[a] The absolute frequencies of the N_2O line centers have been taken from the work of Toth (Ref. 22).

TABLE VI. Summary of the molecular constants of the ν_6 band. Quoted errors are standard deviations in units of the last digit given. All values in MHz.

	$CH_3{}^{79}Br$	$CH_3{}^{81}Br$
ν_6 state		
B	9 534.035 23(66)	9 497.812 65(48)
$D_J \times 10^3$	9.917 17(70)	9.844 79(43)
$D_{JK} \times 10^3$	129.624 (32)	128.807 (22)
$H_J \times 10^6$	− 0.005 217(138)	− 0.004 891(128)
$H_{JK} \times 10^6$	0.066 2 (358)	0.042 9 (58)
$H_{KJ} \times 10^6$	4.433 (194)	5.09 (21)
$\eta_J \times 10^3$	283.430 (88)	282.384 (58)
$\eta_{JK} \times 10^3$	0.036 86(114)	0.032 83(117)
$\nu + A' - B' - 2A\zeta + 3\eta_K/4$	28 703 479.97(25)	28 701 669.96(26)
$A' - B' - A\zeta + \eta_K$	111 964.391(68)	112 017.785 (61)
$A' - B' - A'' + B'' + 3\eta_K/2$	925.077 (42)	924.146 (34)
$D'_K - \eta_K/4 \times 10^3$	1 726.1 (27)	1 720.66 (147)
$D''_K - \eta_K/4 \times 10^3$	1 622.2 (38)	1 639.3 (24)
q_0	− 8.964 7 (33)	− 8.896 3 (18)
$q_1 \times 10^3$	− 0.045 8 (48)	− 0.026 66 (174)
Ground state[a]		
B	9 568.192 793(28)	9 531.830 314(29)
$D_J \times 10^3$	9.872 902(165)	9.801 143(186)
$D_{JK} \times 10^3$	128.656 3 (44)	127.820 4 (63)
$H_J \times 10^6$	− 0.005 627(105)	− 0.005 235(93)
$H_{JK} \times 10^6$	0.109 8 (71)	0.109 8 (93)
$H_{KJ} \times 10^6$	5.950 9 (392)	5.876 (62)

[a] Reference 4.

examine the usefulness of the rotational transitions in the $v_6 = 1$ state, we have removed them from the fit. Three parameters H_{JK}, η_{JK}, and q_1 become undetermined and the standard deviation of the other parameters grows significantly (ten times for D_{JK} and q_0).

DISCUSSION

The parameters determined in this work are significantly more accurate than the previous ones.[2] Two parameters: η_{JK} and q_1 are determined for the first time. All the values are consistent for the two isotopic species and the vibrational dependance is of the expected order of magnitude (except for H'_{JK}, as discussed above). Our $D''_K - \eta_K/4$ and $D'_K - \eta_K/4$ are in reasonable agreement with those of Sakai.[5] Many lines (about one quarter) remain unassigned in the infrared spectrum. Most of these lines belong to the bands $\nu_3 + \nu_6 \leftarrow \nu_3$ and $2\nu_6 \leftarrow \nu_6$ and to the ^{13}C isotopomer. However, some of them are probably high J, high K lines. They were not included into the least-squares fit because, either their experimental intensity was much stronger than expected or several lines lie in the neighborhood so that they could not be assigned by their frequency consistency.

ACKNOWLEDGMENTS

This investigation has been supported in part by the D.R.E.T. and by The Région Nord/Pas-de-Calais.

[1] G. Graner, J. Mol. Spectrosc. **90**, 394 (1981).
[2] F. Herlemont, J. Fleury, J. Lemaire, and J. Demaison, J. Chem. Phys. **76**, 4705 (1982).
[3] M. Ieki, E. Kumamoto, K. Kawaguchi, C. Yamada, T. Tanaka, and E. Hirota, J. Mol. Spectrosc. **71**, 229 (1978).
[4] R. Bocquet, D. Boucher, J. Demaison, G. Wlodarczak, and G. Graner, Europhys. Lett. **2**, 275 (1986).
[5] J. Sakai and M. Katayama, J. Mol. Struct. **190**, 113 (1988).
[6] E. Arimondo, J. G. Baker, P. Glorieux, T. Oka, and J. Sakai, J. Mol. Spectrosc. **82**, 54 (1980).
[7] S. G. Kukolich and C. V. Cogley, J. Chem. Phys. **76**, 1685 (1982).
[8] B. D. Osipov and M. N. Grabois, Opt. Spectrosc. **58**, 702 (1985).
[9] V. J. Corcoran, R. E. Cupp, J. J. Gallagher, and W. T. Smith, Appl. Phys. Lett. **16**, 316 (1970).
[10] V. J. Corcoran, J. M. Martin, and W. T. Smith, Appl. Phys. Lett. **22**, 517 (1973).
[11] G. Magerl, E. Bonek, and W. A. Kreiner, Chem. Phys. Lett. **52**, 473 (1977).
[12] G. Magerl, W. Schupita, and E. Bonek, I.E.E.E. J. Quantum Electron. **18**, 1214 (1982).
[13] S. K. Lee, R. H. Schwendeman, and G. Magerl, J. Mol. Spectrosc. **117**, 416 (1986).
[14] J. Legrand, B. Delacressoniere, J. M. Chevalier, and P. Glorieux, J. Opt. Soc. Am. B (to be published).
[15] A. Dubrulle, J. Burie, D. Boucher, F. Herlemont, and J. Demaison, J. Mol. Spectrosc. **88**, 394 (1981).
[16] C. Freed and A. Javan, Appl. Phys. Lett. **17**, 53 (1970).
[17] K. Sarka, J. Mol. Spectrosc. **39**, 531 (1971).
[18] A. Dubrulle, J. Burie, D. Boucher, F. Herlemont, and J. Demaison, J. Mol. Spectrosc. **88**, 394 (1981).
[19] J. Demaison, A. Dubrulle, D. Boucher, and J. Burie, J. Chem. Phys. **67**, 254 (1977).
[20] T. E. Sullivan and L. Frenkel, J. Mol. Spectrosc. **39**, 185 (1971).
[21] B. Duterage, D. Boucher, J. Burie, J. Demaison, and A. Dubrulle, C. R. Acad. Sci. **284B**, 213 (1977).
[22] R. A. Toth, J. Opt. Soc. Am. B **4**, 357 (1987).